

Antonin VITECEK^a, Andrzej SIOMA^{b,*}, Piotr SULIGA^b, Janusz KOWAL^b

^a Faculty of Mechanical Engineering, VSB Technical University of Ostrava, Czech Republic

^b Faculty of Mechanical Engineering and Robotics, AGH University of Science and Technology, Cracow, Poland

* Corresponding author: sioma@agh.edu.pl

AUTOMATIZATION OF SCREW THREAD PROFILE MEASUREMENT USING A 3D VISION SYSTEM

© 2018 Antonin Vitecek, Andrzej Sioma, Piotr Suliga, Janusz Kowal

This is an open access article licensed under the Creative Commons Attribution International License (CC BY)



<https://creativecommons.org/licenses/by/4.0/>

Key words: 3D image, 3D image analysis, 3D vision system, thread, thread parameters.

Abstract: The purpose of this study is to perform automatic measurement of a screw thread profile acquired with a 3D vision system. Measurements are carried out using a laser triangulation method. The triangulation method requires a calibration procedure to be performed on a measurement stand. The first stage of the calibration procedure allows one to compensate for lens and perspective distortion. Calculated projection model coefficients are also used to transform the image coordinate system into the world coordinate system. Next, a specially designed calibration target with known geometric dimensions is used to position the object's rotation axis on the measurement plane and prepare it for the measurement procedure. This paper presents the algorithms used to perform a measurement for a single cross-section of a screw thread. For the chosen screw thread, the pitch, flank angles, and the radiuses at the crest and root are measured.

Automatyzacja pomiaru wartości profile wkrętaków z wykorzystaniem system wizyjnego 3D

Słowa kluczowe: obraz 3D, analiza obrazu 3D, systemy wizyjne 3D, gwint, parametry gwintu.

Streszczenie: Celem przedstawionych w artykule badań jest przeprowadzenie zautomatyzowanego pomiaru elementu gwintowanego. Pomiar profilu gwintu wykonano przy pomocy systemu wizyjnego 3D opartego na zasadzie triangulacji laserowej. W artykule przedstawiono opis kalibracji stanowiska pomiarowego. Pierwszy etap procedury kalibracyjnej pozwala na kompensację dystorsji układu optycznego oraz zniekształcenia perspektywicznego. Wyznaczone na tym etapie współczynniki macierzy projekcji wykorzystywane są również do transformacji układu współrzędnych obrazu do układu współrzędnych świata. Na kolejnym etapie specjalnie przygotowany cel kalibracyjny, o znanych parametrach geometrycznych, wykorzystany został do wypozycjonowania osi obrotu elementu na płaszczyźnie pomiarowej – wyznaczonej przez wiązkę laserową. W artykule przedstawiono algorytmy wykorzystane podczas wykonywania pomiarów na obrazie pojedynczego przekroju poprzecznego elementu gwintowanego. Przedstawione metody pozwalają na wyznaczenie skoku, kąta zarysu oraz promieni wierzchołka i dna zarysu gwintu.

benefits of incorporating quality control into the production process of a screw thread – the most widely used mechanical element – are numerous. Due to its complex shape, narrow geometrical tolerances, and large-scale production, quality control is not a straight forward process. Over the years, this task has been the focus of much research. Finding a method that is able

Introduction

to guarantee both sufficient resolution and repeatability while being fast enough to control every manufactured element has been the goal of numerous workers in

the scientific community. Conventional methods of controlling a screw thread are performed using mechanical gauges [1], which can quickly differentiate whether the screw is satisfactory or unsatisfactory. Unfortunately, gauges are subject to wear and tear, and in most cases, it is difficult to determine the source of a problem. To get more in-depth, we can use a coordinate measuring machine (CMM), equipped with a needle-like probe [2]. The information provided allows for a detailed measurement of the thread parameters.

Unfortunately, these measurements are time-consuming, and due to the size of the probe, it is not always possible to detect surface level damage. Recently, attention has been given to a technique utilizing CT scans to acquire a three-dimensional cloud of points which represent the thread [3]. Despite high resolutions and the possibility of measuring internal threads, this method has some serious disadvantages, such as the high cost of equipment and long execution times, making it suited to a laboratory rather than on the production line. Another interesting alternative is the use of optical methods [4]. They have all the advantages of non-contact methods, while maintaining high speed and resolution, and they can be based on a 2D or 3D image. In the case of a 3D image, local surface height variations are given directly and every point on the image is assigned with a height value rather than an intensity value. There are a couple of possible approaches on creating a 3D image including stereovision, photometric stereo, shape from focus, shape from texture, and laser triangulation [8]. The last of the listed methods fulfils all the conditions to become an ultimate solution for thread measurement problems. The first part of this paper concentrates on performing the calibration of a measurement stand in order to acquire a thread surface 3D image. In optical methods, acquiring a high quality image is only the first step in the pursuit of a good final result. Properly chosen image analysis techniques are equally significant. According to the National Physics Laboratory, there are seven thread parameters which require control: pitch diameter, major and minor diameter, pitch, flank angles, radius at crest, and radius at root [1]. The second part of this paper includes a detailed explanation of an algorithm for performing measurements of the last four parameters.

1. Performing a calibration of a measurement stand

The calibration procedure is an essential part of preparing every measurement. When it refers to machine vision, it usually consists of three major tasks: The first is to compensate for a lens distortion; the second is to eliminate the perspective, and the third is to scale the image coordinate system into the world coordinate system. If mistakes are made on any of the calibration stages, it leads to erroneous values at the end of the analysis. In this paper, the acquisition of a thread 3D image was performed using a Sick Ranger 3D camera. The calibration procedure of this device involves using a calibration target with one flat side and one sawtooth-shaped side and moving it across the entire camera field of view on the laser plane. Projecting a laser beam on the flat side of the target allows compensation for possible lens distortion. Eliminating perspective and the scaling of the coordinate system is made possible by using the sawtooth-shaped side.

Acquiring a single image from the camera allows the calculation of the height of a single object's cross-section. The element has to be moved with reference to the camera-laser arrangement in order to perform a full surface scanning. There are two possible approaches for creating a mutual motion using either transitional or rotational element motion. Since getting an image of the entire thread surface is only possible with the second method, it was chosen for this paper. Unfortunately, it has its own disadvantages to be dealt with when building a laser triangulation stand. The threaded element has to be rotated around a fixed axis, positioned precisely on the plane defined by the laser beam or camera axis (depending on the camera-laser arrangement). Two examples of erroneous axis alignments are presented in Fig. 1.

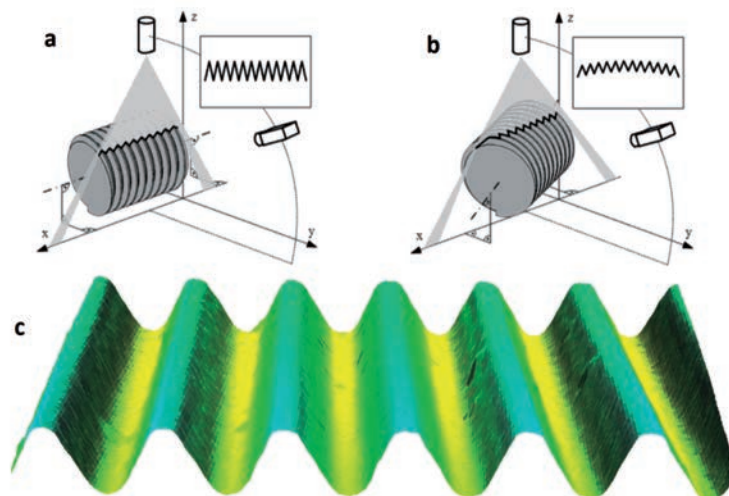


Fig. 1. Measuring stand and picture: a – correct position configuration, b – wrong configuration, c – correct surface image of the thread

In Fig. 1a, an entire thread axis is shifted in one direction with reference to the laser plane. An object profile, visible on the camera image, will be elongated. Performing a correct thread parameter measurement is not possible and will lead to incorrect results. Fig. 1b shows what happens to the camera image when the thread axis is not parallel to the laser beam. The entire object profile is curved and deformed, making it impossible to correctly assess any of the parameters.

One possible solution for this situation is to perform an additional calibration procedure involving a cylinder-shaped calibration target with known geometric dimensions. It should be manufactured with sufficient

precision (depending on the task) and then measured with a CMM. The resolution of such a measurement should be at least an order of magnitude higher than the resolution required by a 3D stand. The calibration target has to have two different diameter values (d_1 , d_2) in order to distinguish a bad axis alignment from a variable distance between the laser and the object. In order to perform a calibration, the cylinder-shaped target has to be mounted in lathe chucks or with another positioning mechanism, which will be used later to set a screw thread in rotational motion. Fig. 2a presents the process of the calibration of the measurement stand.

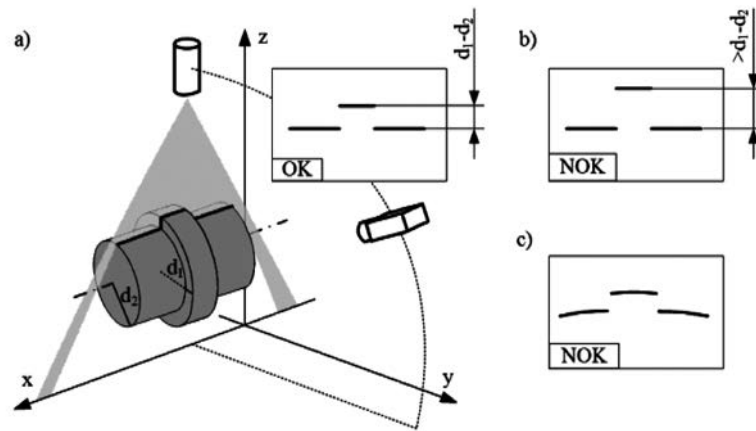


Fig. 2. Performing calibration with cylinder-shaped target

The calibration target has been designed to supply information about the relative position of the rotation axis and the measurement plane. If the calibration target is incorrectly positioned in relation to the vision system, it will be represented on its 3D profile. If the source of an error is analogous to one presented in Fig. 1a, then the height difference between the two parallel lines on the camera image will not match the real values (measured with a CMM) Fig. 2b. An axis rotated in relation to the laser beam plane (as in Fig. 1b) will result in curved lines representing the profile (Fig. 2c). There are a couple of possible approaches to detect these flaws on a mathematical level. One possible solution is to use linear least-squares fitting. This method will be presented in detail in this paper. Our method can be split into three steps. First, the image from the camera has to be processed using line-find algorithms in order to obtain a set of points which represent the profile. This is an extensive topic and will not be covered here. We used a centre of gravity algorithm supplied by the camera software producer. The second step is to segment obtained points into two subsets – one representing the surface of a bigger cylinder d_1 and one representing the surface of a smaller cylinder d_2 . This was presented in

Fig. 3a, where circles represent points of the first data subset and crosses represent points of the second data subset. When this is done, it is possible to perform a least-squares line fitting for both subsets. Vertical linear fit proceeds by finding the sum of the squares of the vertical deviations R^2 of a set of n data points. The minimized functions take the following forms:

$$R_1^2(a_1, b_1) = \sum [y_{i1} - (a_1 + b_1 x_{i1})] \quad (1)$$

$$R_2^2(a_2, b_2) = \sum [y_{j2} - (a_2 + b_2 x_{j2})] \quad (2)$$

where

$R_1^2(a_1, b_1)$ – is a function minimized for a subset of points (x_{i1}, y_{i1}) representing a greater cylinder;

$R_2^2(a_2, b_2)$ – is a function minimized for a subset of points (x_{j2}, y_{j2}) representing a smaller cylinder.

When the minimization is performed, we obtain a linear equation for the greater cylinder surface ($y_{i1} = a_1 x_{i1} + b_1$) and a linear equation for the smaller cylinder surface ($y_{j2} = a_2 x_{j2} + b_2$) Fig. 3a.

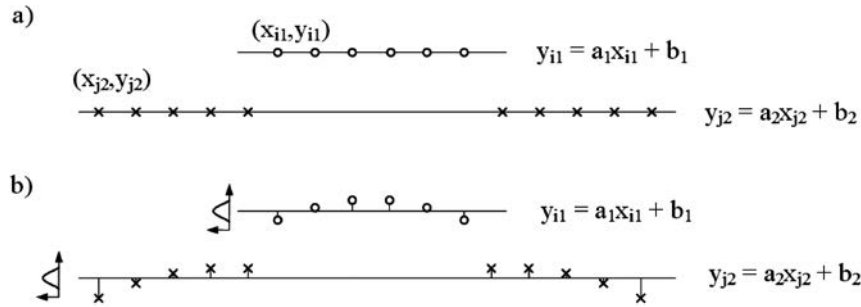


Fig. 3. Detecting an axis misalignment using the cylinder-shaped calibration target image

If the calibration target is perfectly aligned, then “a” parameters for both cylinders should be equal to zero:

$$a_1 = 0, \quad a_2 = 0 \quad (3)$$

The difference between “b” factors should be equal to half the cylinder diameter difference:

$$b_1 - b_2 = \frac{1}{2} (d_1 - d_2) \quad (4)$$

The last condition involves assessing the normal deviation of the vertical distance between subset points and the line calculated using this subset (Fig. 3b). This was done using the following equations:

$$\sigma_1 = \sqrt{\frac{\sum (y_{i1} - \bar{y}_1)^2}{n - 1}} \quad (5)$$

$$\sigma_2 = \sqrt{\frac{\sum (y_{i2} - \bar{y}_2)^2}{m - 1}} \quad (6)$$

In an ideal situation, both normal deviation values should be equal to zero. In the real world, all measurements are subject to noise and thus values will differ from zero. The difficulty is to distinguish errors led by noise from those being the result of an axis misalignment. Assessment of impact made by noise δ_σ was done by repeatedly scanning the same profile of the calibration target surface and calculating a normal deviation value for every point along the profile. This has to be done again for every specific surface, camera-laser arrangement, optical setup, and laser power configuration, since the values can have a significant impact on the results obtained in every specific case. The mean value of calculated normal deviations serves as a threshold for detecting axis misalignment. If one of the values σ_1, σ_2 is greater than δ_σ , axis alignment should be corrected.

$$\sigma_1 \leq \delta_\sigma, \quad \sigma_2 \leq \delta_\sigma \quad (7)$$

When all the conditions given by Eq. 3, Eq. 4, and Eq. 7 are met, the element rotation axis is well positioned with respect to camera-laser arrangement. Now it is possible to mount the threaded element in the same lathe chucks or other positioning mechanism and perform a measurement.

2. Measurement and parameter assessment of a single profile

There are several thread forms in use. Each one of them is characterized by a certain set of parameters. In this paper, we present a method of calculating thread pitch, flank angles, radius at crest, and radius at root for ISO metric screw thread. Different kinds of thread have some common features that make it possible to adapt the presented method to other types of screw threads as well.

Measuring thread parameters involves finding some of its characteristic features. The method presented in this paper can be split into four main stages. The first step requires calculating the positions of the thread roots and crests. There are two possible solutions that may be used depending on a thread type.

If the thread in question has rounded roots or crests (Whitworth thread, knuckle thread), they can be efficiently found using first derivative of the profiles. Since the profile is defined by discrete points rather than a continuous function, the central difference approximation of the first derivative can be used.

$$f'(x_i) = \frac{f(x_{i-1}) - f(x_{i+1})}{2h} \quad (8)$$

Of course, performing a numerical differentiation in such a way amplifies high-frequency noises. Using a median filter before performing differentiation should help to cut out noise without affecting data quality. If the noise value is high compared to a useful signal, we recommend reducing the noise by controlling the environment. Possible causes of high noise values are vibrations of an object or measurement stand, external light sources, too wide laser lines being visible on the

camera sensor, or specular reflections on the object. If introducing any of these improvements do not lead to sufficient data quality, we recommend taking a look at some more advanced methods of performing numerical differentiation as presented in work of Chartrand [5]. The roots and crest of a thread can now be easily found by assessing the intersection point between the profile derivative and the coordinate system x-axis (Fig. 4).

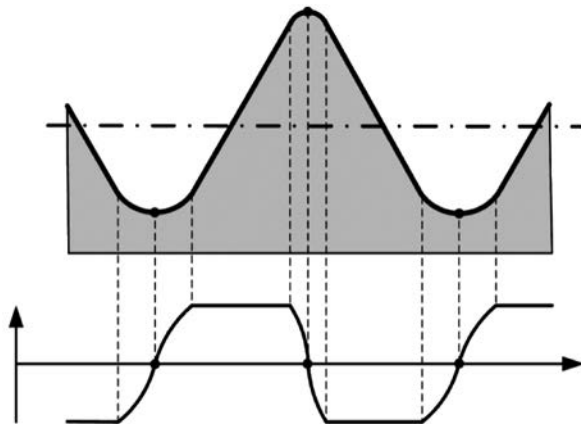


Fig. 4. A thread profile with rounded roots and crest and its derivative

If the crests or roots of a thread are flat, (square thread, Buttress thread), a different approach has to be applied. This involves calculating a centre of gravity of two areas defined by a thread profile and a straight line, and the position of which is calculated using a mean difference value between a crest's heights and a root's heights (Fig. 5). The line position is dependent on a thread type, but it has minor importance. For an ISO screw thread, we can assume that the line is located at $2/5H_N$ from the thread root.

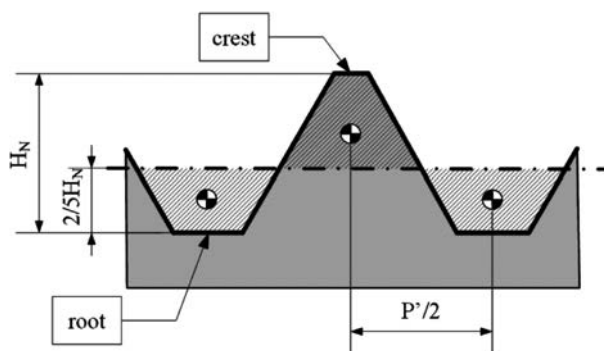


Fig. 5. A thread profile with rounded crests and roots and calculated geometrical centres of selected areas

Regardless of which method was applied in a specific case, a set of coordinates is obtained that represent the positions of roots and crests along a profile (Fig. 6).

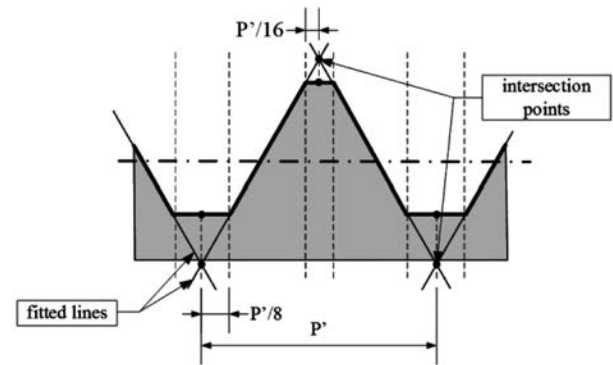


Fig. 6. Algorithm result of line fitting and finding intersection points

Based on the distance between the consecutive roots or crest, we can calculate an approximate value of thread pitch P' . It will be necessary to establish the start and end points of each tooth flank. For an ISO metric thread, each flank should start at approximately $P'/16$ from the profile crest and end at $P'/8$ from the root point. The next step involves fitting straight lines in areas between each starting and ending point as presented in Fig. 7.

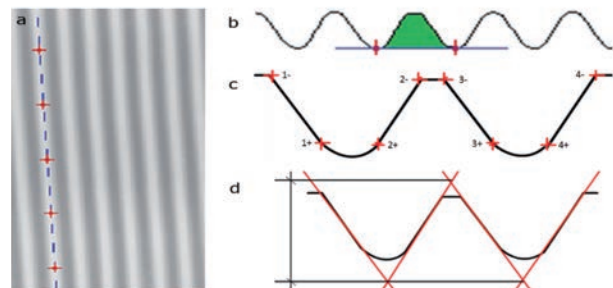


Fig. 7. Sample measurement of thread profile parameters in a 3D image

The minimized function is analogous to those presented in Eq. 1. The only difference is that the set of input points is smaller with each minimization working on a single thread flank. This must be done multiple times. When the calculation is finished, the screw thread flank angle can be easily computed from “a” parameter (linear function slope).

$$\alpha = \arctan(a) \tag{9}$$

Performing a minimization of a distance between real data points representing a flank and straight line can supply one additional piece of information about thread quality. Usually minimization algorithms work with a predefined end value. If the value calculated using Eq. 1 is below a certain limit, the minimization process finishes. If the selected limit value has to be selected from a relatively high value, the thread flanks may be damaged in some way (scratches, grooves, cavities).

The third step is to calculate the intersection points of the lines representing neighbouring flanks. In previous work done by Latypov [5], thread pitch was calculated by fitting a circle between profile flanks. This method is based on the widely used tactile thread measurement method of using three wires. Unfortunately, it requires some initial knowledge about the thread. The fitted circle diameter has to be known in advance based on expected pitch value. Based on our observations, measuring a distance between previously calculated intersection points does not give results that vary much from those calculated based on the Latypov method. The advantage is that no preliminary knowledge is necessary to perform a measurement, so the potential for human error is minimized in this case.

The fourth stage of our calculations allows us to assess the value of a radius at crest and root. In some kinds of threads, measuring these parameters does not lead to any meaningful information. An ISO metric thread often has flattened crests, but for other kinds of thread – for example round threads – both radius values are equally important in order to work properly. In order to obtain a radius value, we have to fit a circle into the section of thread representing the root or crest. Those sections are defined in a similar way to those used for line fitting. The circle fitting algorithm is based on the method described by Gander, Golub, and Strebel [6],

if the requested circle is described in the following parametric form:

$$x = z_1 + r \cos \varphi, y = z_2 + r \sin \varphi \quad (10)$$

The points representing a root or a crest are given as $P_i(x_{i1}, x_{i2})$, so the function that has to be minimized and takes the following form:

$$\sum_{i=1}^m \left\{ \min_{\varphi_i} \left[(x_{i1} - x(\varphi_i))^2 + (x_{i2} - y(\varphi_i))^2 \right] \right\} \quad (11)$$

As a result of the algorithm, we get a radius value for one selected root or crest. To get the parameters for the entire thread, the operation should be repeated.

The outline analysis allows for automatic detection of defects in the profile created during the thread forming process. Figure 7 presents a three-dimensional image with marked defect areas. Regardless of the type of the defect, the allowance for the loss of material during the measurement is visible as a disturbance of the correct profile. The visibility of the defects depends on the resolution of the 3D vision system, the thread size, and the size of the imaging field. Increasing the field of imaging results in a reduction in the size of defects and, consequently, in the possibility of detecting them.

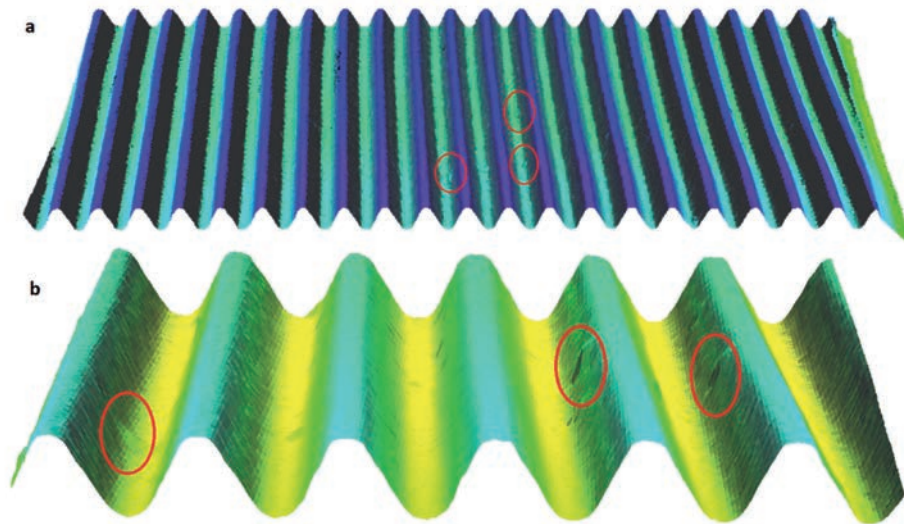


Fig. 8. Thread surface with marked areas of profile defects

Conclusion

The presented method is a good possible solution to solve the screw thread quality control conundrum. It can be implemented on a production line to control every produced threaded element and meets all requirements in terms of speed, accuracy, and overall capabilities.

The presented calibration algorithm, using a cylinder-shaped calibration target, is straightforward but can easily ensure that the positioning of the measured object is correct with respect to the measurement unit.

Currently, screw thread quality control is only done on selected elements from a single batch. Moreover, the information obtained is purely binary (the element is either simply good or not good), and identifying

the source of the problem is difficult. Acquiring an image of a thread surface using laser triangulation and then assessing its parameters with the mathematical algorithms presented in this paper allows us to get more comprehensive information about the production process. Future research will involve comparing these obtained results with data from other measuring techniques such as CMM.

From the point of view of conducting quality control in the manufacturing of threads, there is an interesting possibility of combining the description of the thread profile parameters with evaluations of the thread surface. The thread may have the correct parameters of the profile, but it is still possible that it will have surface defects which disqualify its technical use.

References

1. NPL Notes on Screw Gauges. National Physical Laboratory. Great Britain, 2007.
2. Carmignato S., De Chiffre L.: A New Method for Thread Calibration on Coordinate Measuring Machines. *CIRP Annals – Manufacturing Technology*, 2003, 52(1), pp. 447–450.
3. Kosarevsky S., Latypov V.: Detection of Screw Threads in Computed Tomography 3D Density. *Measurement Science Review*, 2013, 13(6), pp. 292–297.
4. Mutambi J., Li-jun Y.: Application of Digital Image Analysis Method in Metric Screw Thread Metrology. *Journal of Shanghai University*, 20014, 8(2), pp. 208–212.
5. Kosarevsky S., Latypov V.: Development of an algorithm to detect screw threads in planar point clouds. *Measurement Science Review*, 2010, 10(4), pp. 136–141.
6. Chartrand R.: Numerical Differentiation of Noisy, Nonsmooth Data. *ISRN Applied Mathematics*, 2011, Article ID 164564.
7. Gander W., Golub G., Strebel R.: Least-Squares Fitting of Circles and Ellipses. *BIT Numerical Mathematics*, 1994, 34(4), pp. 558–578.
8. Sioma A.: The estimation of resolution in 3D range image system. In: *International Carpathian Control Conference (ICCC)*, Rytro (Poland), May 2013. *IEEE*, 2013, pp. 346–349.

